

## ORIGINAL ARTICLE

# LRIG1 modulates aggressiveness of head and neck cancers by regulating EGFR-MAPK-SPHK1 signaling and extracellular matrix remodeling

JJ-C Sheu<sup>1,2,3</sup>, C-C Lee<sup>4</sup>, C-H Hua<sup>5</sup>, C-I Li<sup>4</sup>, M-T Lai<sup>6,7</sup>, S-C Lee<sup>8</sup>, J Cheng<sup>1</sup>, C-M Chen<sup>1</sup>, C Chan<sup>1</sup>, SC-C Chao<sup>1</sup>, J-Y Chen<sup>4</sup>, J-Y Chang<sup>4</sup> and C-H Lee<sup>4</sup>

EGFR overexpression and chromosome 3p deletion are two frequent events in head and neck cancers. We previously mapped the smallest region of recurrent copy-number loss at 3p12.2–p14.1. *LRIG1*, a negative regulator of EGFR, was found at 3p14, and its copy-number loss correlated with poor clinical outcome. Inducible expression of *LRIG1* in head and neck cancer TW01 cells, a line with low *LRIG1* levels, suppressed cell proliferation *in vitro* and tumor growth *in vivo*. Gene expression profiling, quantitative RT-PCR, chromatin immunoprecipitation, and western blot analysis demonstrated that *LRIG1* modulated extracellular matrix (ECM) remodeling and EGFR-MAPK-SPHK1 transduction pathway by suppressing expression of EGFR ligands/activators, MMPs and SPHK1. In addition, *LRIG1* induction triggered cell morphology changes and integrin inactivation, which coupled with reduced *SNAIL2* expression. By contrast, knockdown of endogenous *LRIG1* in TW06 cells, a line with normal *LRIG1* levels, significantly enhanced cell proliferation, migration and invasiveness. Such tumor-promoting effects could be abolished by specific MAPK or SPHK1 inhibitors. Our data suggest *LRIG1* as a tumor suppressor for head and neck cancers; *LRIG1* downregulation in cancer cells enhances EGFR-MAPK-SPHK1 signaling and ECM remodeling activity, leading to malignant phenotypes of head and neck cancers.

*Oncogene* (2014) 33, 1375–1384; doi:10.1038/onc.2013.98; published online 29 April 2013

**Keywords:** *LRIG1*; head and neck cancers; EGFR; MAPK; SPHK1; ECM remodeling

## INTRODUCTION

Nasopharyngeal carcinoma (NPC) and oral squamous cell carcinoma (OSCC) are two major subtypes of head and neck cancers. Genetic susceptibility, viral infection and chemical exposure have been suggested as risk factors for development of these human malignancies.<sup>1</sup> Enhanced genome instability with gross chromosomal abnormalities has been directly correlated with tumor recurrence and metastasis of NPC,<sup>2,3</sup> leading to high mortality and low five-year overall survival, which have not been improved in decades.<sup>4</sup> Understanding of the molecular mechanisms involved in the development of advanced head and neck cancers will help in clinical management and drug discovery. Genome-wide surveys and clinical association studies have identified two recurrent copy-number aberrations, 3p deletion (3p12.3–p14.2) and 3q amplification (3q26.2–26.32), with prognostic value for metastatic NPC.<sup>3</sup> Notably, chromosome 3p loss is also a genetic hallmark in other types of head and neck cancers<sup>5,6</sup> and has been defined as a crucial early event in NPC progression.<sup>7</sup> These findings suggest that potent tumor suppressors may be encoded within the 3p deletion region, 3p12.3–p14.2.

*LRIG1*, a negative regulator of EGFR mapping to 3p14, encoding a transmembrane protein containing fifteen leucine-rich repeats and three Ig-like domains in its extracellular region, has been

proposed as a tumor suppressor gene,<sup>3,8</sup> and shown to be downregulated in several tumor types, for example, renal cell carcinoma,<sup>9</sup> advanced cervical cancer,<sup>10</sup> glioma<sup>11</sup> and breast cancer.<sup>12,13</sup> In addition, *LRIG1* downregulation correlates with higher tumor grade and a worse outcome in human squamous cell carcinoma<sup>14</sup> and breast cancer.<sup>15</sup> Currently, the tumor suppressive function of *LRIG1* is mainly attributed to its inhibitory effect on EGFR signaling. Over the past few years, it has been shown that *LRIG1* binds to EGFR and attenuates EGFR signaling via both receptor degradation and catalytic inhibition.<sup>16</sup> Moreover, soluble ectodomains of *LRIG1* are sufficient to reduce EGFR activity via shedding of the leucine-rich repeats region and Ig-like domains.<sup>17,18</sup> Ectopic expression of *LRIG1* on the other hand, inhibits cancer cell motility and invasiveness of EGFR (+) prostate cancer cells<sup>19</sup> and EGFRvIII (+) glioblastoma cells.<sup>11,20</sup> Besides ErbB family, functions of other receptor tyrosine kinases like Met and Ret have been reported to be regulated by *LRIG1* via cbl-independent degradation mechanism.<sup>21,22</sup> These findings imply that *LRIG1* may have an anti-metastatic role in human cancers.

Although constitutive activation or overexpression of EGFR is frequently found in head and neck cancers,<sup>23,24</sup> molecular mechanisms underlying functional roles of *LRIG1* in head and neck cancer remain elusive. The present study demonstrates

<sup>1</sup>Human Genetic Center, China Medical University Hospital, Taichung, Taiwan; <sup>2</sup>School of Chinese Medicine, China Medical University, Taichung, Taiwan; <sup>3</sup>Department of Health and Nutrition Biotechnology, Asia University, Taichung, Taiwan; <sup>4</sup>National Institute of Cancer Research, National Health Research Institutes, Zhunan Town, Taiwan; <sup>5</sup>Department of Otolaryngology, China Medical University Hospital, Taichung, Taiwan; <sup>6</sup>Department of Pathology, Chung Shan Medical University Hospital, Taichung, Taiwan; <sup>7</sup>School of Medicine, Chung Shan Medical University, Taichung, Taiwan and <sup>8</sup>College of Medical Science and Technology, Chung Shan Medical University, Taichung, Taiwan. Correspondence: Dr C-H Lee, National Institute of Cancer Research, National Health Research Institutes, R2, R1211, Keyan Road, Zhunan Town 35053, Taiwan or Dr JJ-C Sheu, Human Genetic Center, Cancer Genomics Lab, China Medical University Hospital, 2 Yuh-Der Road, Taichung 40447, Taiwan.

E-mail: chlee124@nhri.org.tw or jimsheu@mail.cmu.edu.tw

Received 28 June 2012; revised 29 January 2013; accepted 1 February 2013; published online 29 April 2013

LRIG1 expression as significantly lower in NPC and OSCC tumors than in their non-tumor counterparts. Lower LRIG1 levels in NPC patients are prognostic for poor survival. Using a Tet-off inducible system in NPC cells, we demonstrated anticancer effects both *in vivo* and *in vitro*, triggered by LRIG1 induction. Using cDNA microarrays, we probed the signaling network regulated by LRIG1 expression in head and neck cancers, with validated results by chromatin immunoprecipitation (ChIP), antibody array, western blot and fluorescent immunostaining. To mimic clinical conditions, we examined oncogenic effects of LRIG1 loss in NPC cells by siRNA knockdown. Finally, we provide evidence that malignant behavior of LRIG1 knockdown cells was greatly decreased by treatment with specific inhibitors against components of the EGFR-MAPK-SPHK1 signaling pathway.

## RESULTS

LRIG1 downregulation correlates with EGFR activation and poor clinical outcome in human head and neck cancers

Our previous study found a significant association between *LRIG1* deletion and poor clinical outcome in NPC patients.<sup>3</sup> To examine LRIG1 protein levels, we performed immunohistochemistry on tissue microarrays containing 44 metastatic NPC tumor samples. LRIG1 immunoreactivity was very intense in adjacent non-tumor epithelium, but only weakly positive in 65.9% (29 of 44) and undetectable in 34.1% (15 of 44) NPC samples (Figure 1a). Though no correlation emerged between LRIG1 loss and total EGFR levels (data not shown), NPC tumors with undetectable LRIG1 had higher phospho-EGFR (pEGFR) levels than those with positive LRIG1 staining (86.7 vs 13.8%,  $P < 0.001$ , Figure 1a), portending a negative regulatory role of LRIG1 in EGFR signaling. Kaplan–Meier survival analysis indicated a significant correlation ( $P = 0.038$ ) between low levels of LRIG1 and poor clinical outcome: NPC patients with positive LRIG1 staining exhibited a longer median survival time (108.6 months) than those with undetectable LRIG1 (33.8 months) (Figure 1b). In agreement with these findings for NPC, cDNA microarray data from OSCC samples showed

reduced LRIG1 expression in tumors compared with adjacent non-tumor epithelium ( $P < 0.001$ ) (Figure 1c).

Next, we analyzed LRIG1 protein levels in head and neck cancer cell lines by western blot. Supplementary Figure S1 shows LRIG1 markedly downregulated in five NPC and four OSCC cell lines tested compared with the non-transformed nasopharyngeal NP460hTert and oral CGHNK6 cells. These indicate that LRIG1 downregulation is common in head and neck cancer patients, along with bad prognosis. LRIG1 deletion may trigger oncogenic signals promoting the development of head and neck cancers.

LRIG1 induction in NP cells reduces cell growth *in vitro* and tumorigenicity *in vivo*

To characterize the role of LRIG1 in head and neck cancers, we established stable Tet-off inducible clones in TW01 cells, with LRIG1 expression barely detectable (Supplementary Figure S1). Western blots confirmed that LRIG1 expression could be turned on/off under the control of tetracycline-response element in clones TW01-LG1/a and TW01-LG1/b (Figure 2a). Tetracycline cannot induce the expression of LRIG1 in vector transfectants (Supplementary Figure S2). The LRIG1 expression level of TW01-LG1/b cells is much higher than those of the untransformed NP460hTert cells. So we used TW01-LG1/a cells, which have a near normal LRIG1 expression level, for experiments. Figure 2b shows that LRIG1 induction significantly reduced the proliferation rate of TW01-LG1/a cells as early as 24 h after LRIG1 induction. Cell cycle analysis and annexin V staining indicated a tendency of G2/M arrest triggered by LRIG1 expression (Supplementary Figure S3a), which led to the accumulation of cells in the sub-G1 population and cell death (Supplementary Figure S3b). To determine whether LRIG1 controls tumor growth *in vivo*, we used a xenograft model in immunocompromised (*nu/nu*) mice by injecting subcutaneously with TW01-LG1/a cells and found that, compared with the non-induced group (LRIG1 off), LRIG1-expressing tumors (LRIG1 on) showed a much slower growth rate (Figure 2c) and lower tumor weight ( $P = 0.008$ , Figure 2d). On the other hand, we turned on

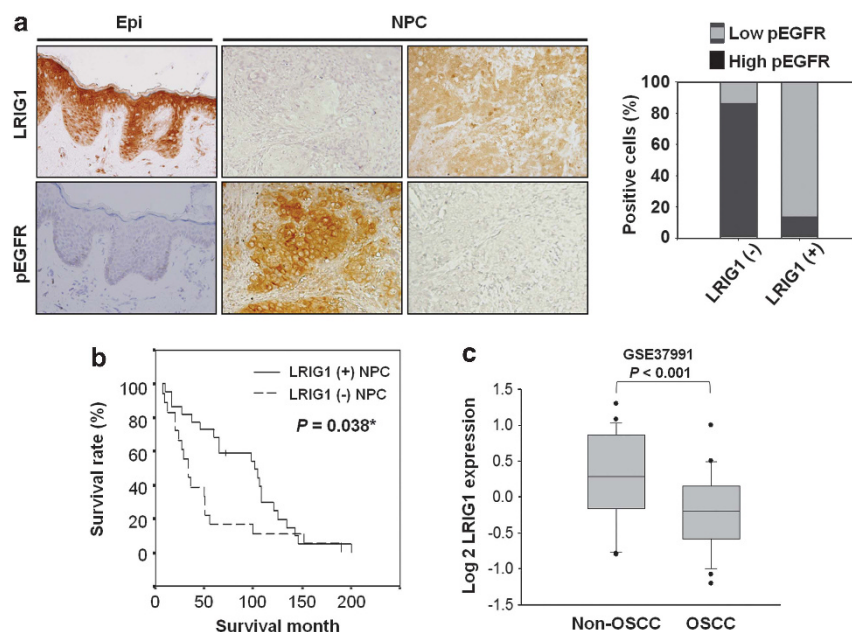


**Figure 1.** LRIG1 expression in head and neck tumors and clinical association analysis. (a) Immunohistochemistry for LRIG1 (upper panel) and phospho-EGFR (pEGFR, lower panel) was performed on tissue microarray sections containing NPC samples (NPC) and normal nasal epithelium (Epi). The bar chart at the right panel plots percentage of cells with weak or high staining for pEGFR in the LRIG1 (+) and LRIG1 (-) samples. (b) Overall survival of LRIG1 (+) and LRIG1 (-) NPC patients was compared by Kaplan–Meier survival analysis. (c) LRIG1 expression in 28 OSCC tumors and matched non-tumor tissues (GSE37991).

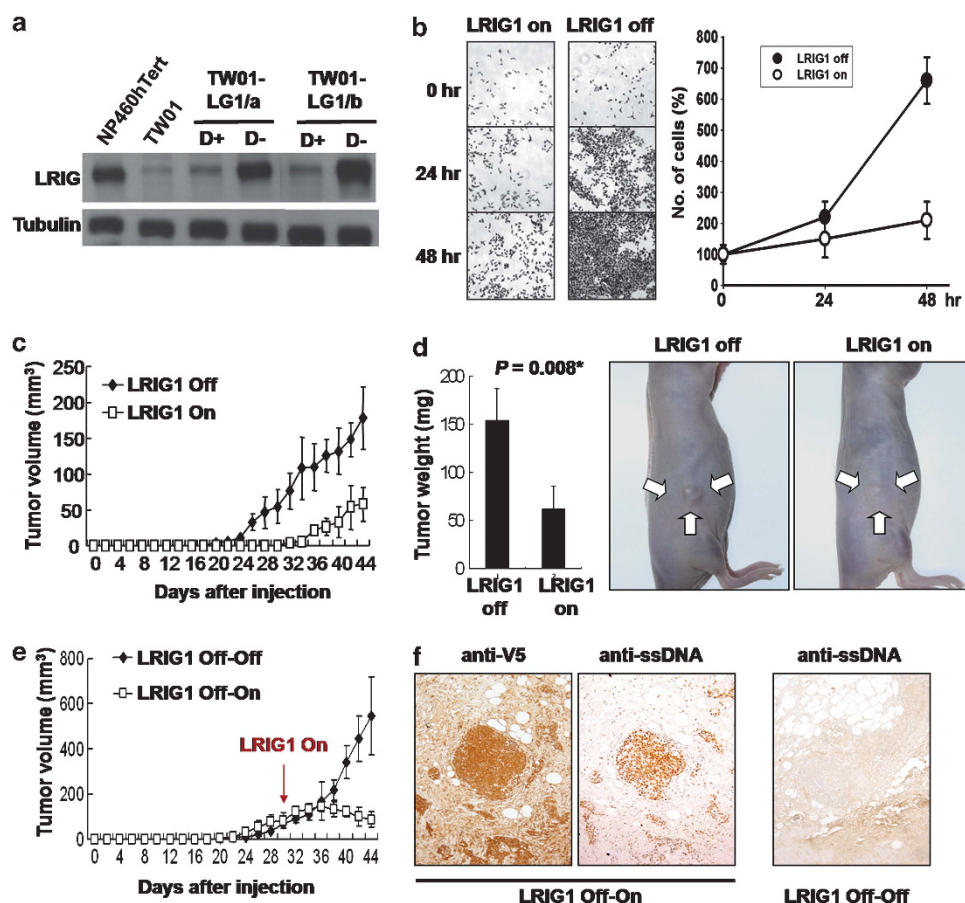


**Figure 2.** LRIG1 expression inhibits tumor cell growth *in vitro* and *in vivo*. **(a)** Western blot confirms regulation of LRIG1 expression by the Tet-off vector system with (D+) or without (D-) doxycycline. NP460hTert and TW01 parental cells served as the positive and negative control, respectively. **(b)** *In vitro* growth analysis of TW01-LG1/a cells under LRIG1 turned-off and turned-on conditions. Left panel: representative images show inhibitory effect of LRIG1 expression on NPC cell growth. Right panel: cell numbers were assessed by MTT assay and expressed as percentage of cell numbers at time zero. The data represent mean  $\pm$  s.d. from three independent experiments, each with four replicates. **(c–f)** A tumor xenograft experiment was performed on athymic nu/nu mice by subcutaneously injecting LRIG1-inducible TW01-LG1/a cells. Induction of LRIG1 expression was performed on Day 1 (**c, d**) or Day 30 (**e, f**) post injections. **(c and e)** Tumor volume was measured with time. **(d)** Representative photographs of tumors for each group were taken on Day 40 with the average tumor weight on Day 43. Data indicate mean tumor weight  $\pm$  s.d.,  $n = 6$ . **(f)** IHC studies using specific Abs against single-stranded DNA (anti-ssDNA) revealed apoptosis induction in tumor cells, which re-expressed LRIG1 (anti-V5) in LRIG1 off-on group. Tumors from LRIG1 off-off group served as the negative control.

LRIG1 expression in mice carrying xenografted tumors at Day 30 post injection (LRIG1 off-on), and found that tumor size did not increase or even shrink 2 weeks (14 days) after LRIG1 induction, as compared with LRIG1 non-inducing tumors (LRIG1 off-off) (Figure 2e). IHC using specific Abs against single-stranded DNA (anti-ssDNA), which marked apoptotic instead of necrotic cells, indicated apoptosis induction in cells overexpressing LRIG1 (Figure 2f), which may lead to tumor regression.

LRIG1 has negative regulatory roles in oncogenic signaling by downregulation of EGFR ligands and SPHK1

To identify cancer-related genes and pathways regulated by LRIG1, we performed time-course microarray experiments with TW01-LG1/a cells during the period of LRIG1 induction. Significant transcriptional change was found 36 h after LRIG1 was turned on. Venn diagram analysis showed 46 genes overlapping with either an ascending or descending trend in mRNA expression level (Figure 3a), which could be further validated by quantitative RT-PCR (Figures 3c and 4a and Table 1). Functional annotation analysis by PANTHER classification system (<http://www.pantherdb.org>) indicated diverse targets regulated by LRIG1 at transcriptional level (Figure 3b and Table 1). In addition to enhancing EGFR degradation, the transcription of EGFR ligands/activators, such as amphiregulin (AREG), neuregulin 1

(NRG1), transforming growth factor- $\alpha$  (TGFA), and heparin-binding EGF-like growth factor (HBEGF), was reduced in response to LRIG1 induction (Figures 3b and c). Consistent with prior findings,<sup>16,19</sup> LRIG1 induction was accompanied in a time-dependent manner by enhancing EGFR degradation and reducing phosphorylation of EGFR and MAPK (Figure 3d). Expression of sphingosin kinase 1 (SPHK1), a downstream target of MAPK,<sup>25</sup> was also reduced by LRIG1 induction (Figure 3d).

LRIG1 inhibits extracellular matrix remodeling by downregulation of SNAI2 and MMPs

Microarray experiments also revealed several genes involved in extracellular matrix (ECM) remodeling, such as those coding for MMP-1, MMP-3, MMP-10, MMP-12, MMP-13, ITGA2, LAMB3, AMIGO2 and GJB5, accounting for the major group of LRIG1 targets (Figures 3b and 4a, and Table 1). Notably, expression of epithelial-to-mesenchymal transition marker SNAI2 was also reduced (Figures 3d and 4a), suggesting that LRIG1 has a role in ECM remodeling. Subsequent western blot analysis using anti-MMP antibody array demonstrated a reducing trend of several MMPs at protein level, including MMP-1, MMP-2, MMP-3, MMP-8, MMP-9, MMP-10 and MMP-13, upon LRIG1 being turned on. Supplementary Figure S4 shows whole images of MMP protein



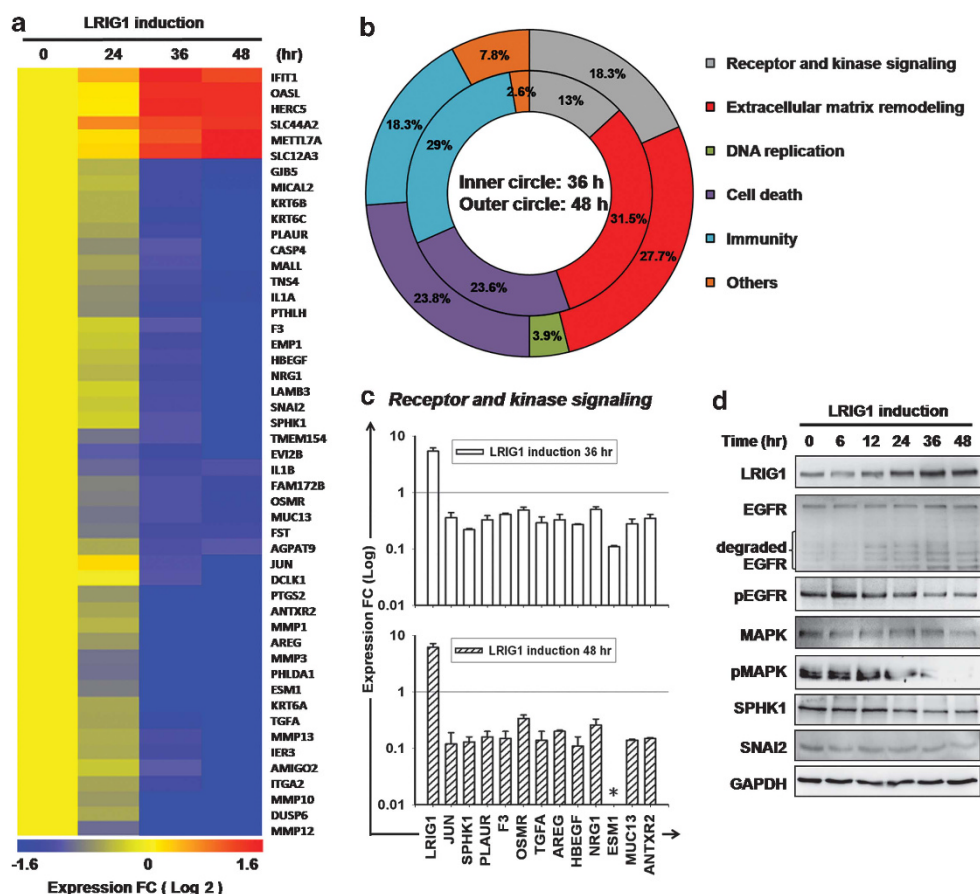


**Figure 3.** Transcriptomic regulation by LRIG1 induction. **(a)** Hierarchical clustering shows differentially expressing genes at 24, 36 and 48 h following LRIG1 being turned on. Level of gene expression at time zero (LRIG1 turned-off) was assigned as the basal level for each gene; red indicates upregulation and blue indicates downregulation of gene expression. **(b)** Functional classification of LRIG1 transcriptional targets using the PANTHER classification system (<http://www.pantherdb.org>). **(c)** Quantitative RT-PCR analysis of the LRIG1-regulated genes involved in receptor and kinase signaling. **(d)** Western blot shows that LRIG1 induction enhances EGFR degradation, but inhibits phosphorylation of EGFR and MAPK as well as the expression of SPHK1 and SNAI2. Cells were lysed at the indicated times after LRIG1 was turned on. GAPDH served as the loading control.

arrays at different color-development time points. Interestingly, the level of TIMP2, an MMP inhibitor, was significantly increased (Figure 4b). As phospho-MAPK (pMAPK) can be translocated into cell nucleus and act as a transcriptional regulator,<sup>26</sup> we examined whether pMAPK was directly responsible for reduced expression of LRIG1 targets. Chromatin immunoprecipitation (ChIP) analysis with anti-pMAPK antibodies revealed that LRIG1 induction significantly attenuates binding of pMAPK-associated transcription factors to promoter regions of MMP-1, MMP-3 and MMP-10 (Figure 4c). This finding suggests a novel transcriptional role of LRIG1 in regulating the expression of ECM factors, at least in part mediated via transcriptional regulation by pMAPK. Subsequent cell morphology analyses revealed a spread-out squamous cell shape in LRIG1 turned-on cells as compared with spindle-like shape in LRIG1 turned-off cells (Figure 4d). Immunofluorescence staining revealed activated integrin (Figure 4e), a hallmark of active ECM remodeling, in LRIG1 turned-off, but not in LRIG1 turned-on cells. These results support a regulatory role of LRIG1 in ECM remodeling.

LRIG1 knockdown promotes oncogenicity, which can be suppressed by MAPK and SPHK1 inhibitors

According to our findings, we proposed that the aggressiveness of cancer cells caused by LRIG1 loss might be suppressed by treatment with MAPK or SPHK1 inhibitors. To test this hypothesis,

we used specific siRNA (siLRIG1) to knockdown LRIG1 expression in TW06 cells, which showed the highest LRIG1 levels among head and neck cancer cell lines tested (Supplementary Figure S1). Western blot confirmed the robust effect of siLRIG1 on LRIG1 expression and that levels of pEGFR, pMAPK, SPHK1, and SNAI2 were all raised by LRIG1 knockdown (Figure 5a). Increased SNAI2 levels and decreased E-cadherin levels (Figure 5a) support the finding that cells with low LRIG1 expression have a spindle-like shape, while those with high LRIG1 levels have a squamous cell-like shape (Figure 4d). Anchorage-independent growth assay showed more and larger colonies formed by cells transfected with siLRIG1 than those transfected with scrambled control (Figure 5b), suggesting that LRIG1 downregulation led to the acquisition of survival advantages in head and neck cancer cells. Interestingly, such effect was significantly decreased by treatment with MAPK inhibitor U0126 or SPHK1 inhibitor SK1-I (Figure 5b). Although U0126 treatment slightly inhibits the clonogenicity of scrambled control cells, SK1-I has no effect on TW06 cells (Figure 5b). Transwell migration (Figure 5c) and invasiveness (Figure 5d) were significantly enhanced by LRIG1 knockdown, and these effects were both markedly inhibited by U0126 or SK1-I. Treatment of U0126 and SK1-I had no significant inhibitory effect on the migration and invasion of the scrambled control cells. It should be noted that, at the concentrations used (3  $\mu$ M), U0126 or SK1-I had only a minor or undetectable cytotoxic effect on TW06 cells

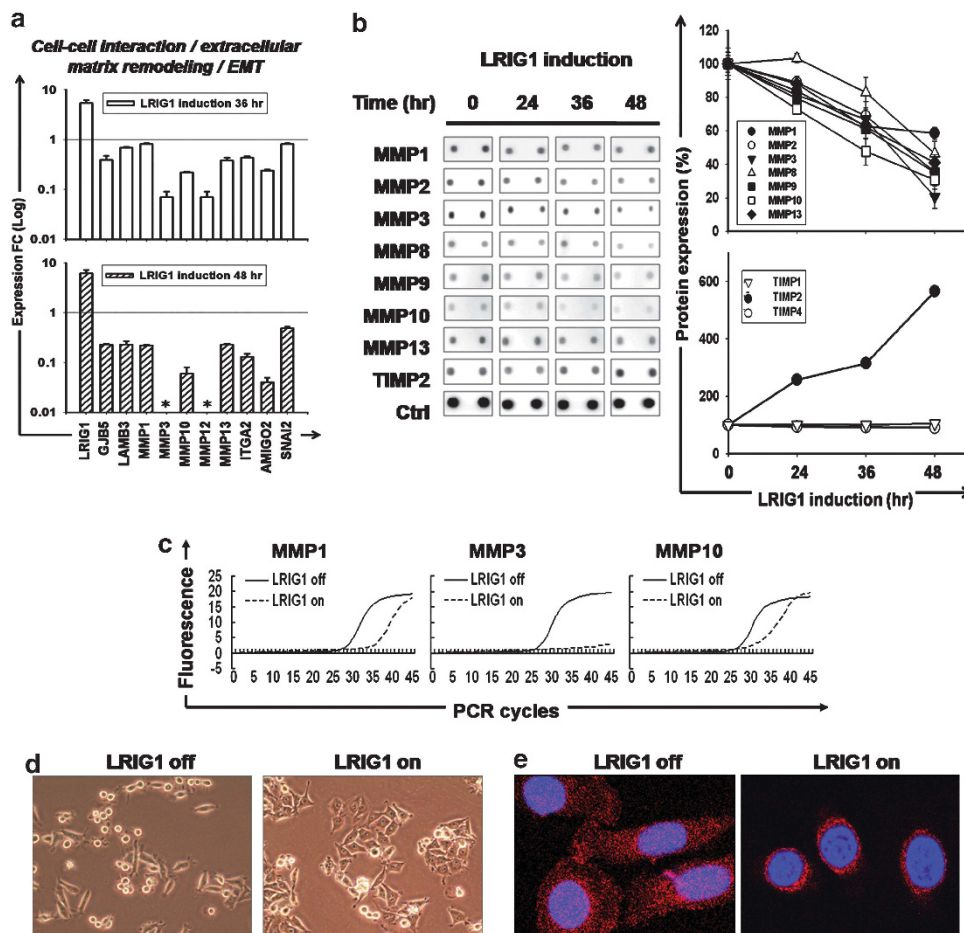


**Figure 4.** LRIG1 attenuates ECM remodeling by downregulation of SNAI2 and MMPs. **(a)** Quantitative RT-PCR analysis of LRIG1-regulated genes involved in cell-cell interaction, ECM remodeling and epithelial-to-mesenchymal transition. **(b)** Metalloproteinase antibody arrays were utilized to detect protein levels of MMPs and TIMPs at indicated time points. Intensity of each spot was quantified using an ImageQuant LAS4000 and normalized to that of the positive controls (original images of hybridized MMP array could be found in Supplementary Figure S4). Plots at the right panel summarize protein dynamics of MMPs (upper) and TIMPs (lower) after LRIG1 induction in TW01-LG1/a cells. Lysates collected at 0 h served as the 100% level in all experiments. **(c)** ChIP data in LRIG1 turned-on and turned-off cells were validated by ChIP-qPCR. ChIP analysis was performed with anti-pMAPK. Upon LRIG1 induction, the content of pMAPK in TW01-LG1/a cells decreased, thus reduced the binding capability of pMAPK-associated transcription factors towards the promoter region of *MMP-1*, *MMP-3* and *MMP-10*. **(d)** NPC cells display distinct morphologies under LRIG1 turned-on and turned-off conditions for 24 h (phase-contrast images at  $\times 400$  magnification). Cells were grown on collagen-coated dishes, as described in Materials and methods. **(e)** Fluorescent immunostaining indicates integrin- $\beta 1$  inactivation in cells with LRIG1 turned-on for 24 h. Staining with LRIG1 turned-off cells reveal visible cytoplasmic and membrane localization, suggesting active ECM remodeling activity.

(Supplementary Figure S5). In addition, empty vector transfectant derived from TW01 (TW01-Vec) showed no change in protein levels of pMAPK and SPHK1 after removal of doxycycline (Supplementary Figure S2). These findings suggest that loss of LRIG1 expression is the major cause of MAPK and SPHK1 activation. To confirm results from culture experiments, we performed IHC staining against SPHK1 or pMAPK with graft tumors. Although tumors in LRIG1 turned-on group gradually lost LRIG1 expression after long-term clonal evolution, IHC results showed lower immunointensity of anti-SPHK1 and anti-pMAPK in the LRIG1-positive area than the ones in surrounding LRIG1-negative tissue (Supplementary Figure S6). Our results support a cross-talk among EGFR, MAPK and SPHK1 that are regulated by LRIG1, and prove the association of LRIG1 downregulation with aggressiveness of head and neck cancers.

## DISCUSSION

The present study provides the first evidence that LRIG1 downregulation promotes malignant characteristics in head and neck

cancers by enhancing EGFR-MAPK-SHPK1 signaling and the associated ECM remodeling activity. Our data also demonstrate that LRIG1 downregulation serves as a prognostic marker for aggressive NPC (Figure 1b). A Tet-off inducible system revealed MMPs and SPHK1 as direct downstream targets of LRIG1 and that the induction of LRIG1 is associated with low SPHK1 and MMP expression (Figures 3 and 4, and Table 1). In addition, LRIG1 was shown to regulate transcription by reducing the expression of pMAPK and possibly other transcriptional factors (Figure 4c). The increased expression of LRIG1 changed gene expression profiles, leading to a dynamic shift in the cellular signaling network from oncogenic to tumor-suppressing (Figure 3a). These findings might explain why LRIG1 knockdown conferred advantages for tumor growth in mice, with larger tumors being seen in the LRIG1-off than in the LRIG1-on group (Figures 2c and d).

Based on our data, we proposed a model for the role of LRIG1 in a positive feedback inhibitory loop in EGFR-MAPK-SPHK1 signaling and ECM remodeling (Figure 6). In the presence of LRIG1, activation of EGFR and MAPK is attenuated, thus reducing transcription of EGFR ligands/activators by lowering levels of

**Table 1.** List of common differentially expressed genes at 36 h and 48 h after LRIG1 induction

Symbol	Accession no.	Molecular function <sup>a</sup>	Gene description	FC (array)		FC (qPCR)	
				36 h	48 h	36 h	48 h
Receptor and kinase signaling							
JUN	NM_002228	Transcription activity and cell cycle	Jun oncogene	0.24	0.10	0.36	0.12
SPHK1	NM_021972	Receptor protein tyrosine kinase signaling pathway	Sphingosine kinase 1	0.24	0.12	0.22	0.13
PLAUR	NM_002659	Receptor activity	Plasminogen activator, urokinase receptor	0.19	0.11	0.33	0.16
F3	NM_001993	Cytokine receptor activity	Coagulation factor III	0.24	0.09	0.41	0.15
OSMR	NM_003999	Cytokine receptor activity	Oncostatin M receptor	0.23	0.18	0.49	0.34
TGFA	NM_003236	Growth factor activity	Transforming growth factor, alpha	0.16	0.06	0.29	0.14
AREG	NM_001657	Growth factor activity	Amphiregulin	0.11	0.02	0.33	0.20
HBEGF	NM_001945	Growth factor activity	Heparin-binding EGF-like growth factor	0.22	0.09	0.27	0.11
NRG1	NM_001160002	Growth factor activity	Neuregulin 1	0.20	0.08	0.50	0.26
ESM1	NM_007036	Growth factor activity	Endothelial cell-specific molecule 1	0.08	0.07	0.11	0.01
MUC13	NM_033049	Receptor activity; receptor binding	Mucin 13, cell surface-associated	0.23	0.18	0.28	0.14
ANTXR2	NM_058172	Receptor activity	Anthrax toxin receptor 2	0.13	0.04	0.35	0.15
Cellular stress and apoptosis							
CASP4	NM_001225	Apoptosis and proteolysis	Caspase 4	0.24	0.13	0.75	0.51
EMP1	NM_001423	Apoptosis	Epithelial membrane protein 1	0.20	0.09	0.37	0.18
DUSP6	NM_022652	Oxidative stress response	Dual specificity phosphatase 6	0.09	0.01	0.19	0.03
AGPAT9	NM_032717	Calcium-dependent phospholipid binding	1-acylglycerol-3-phosphate O-acyltransferase 9	0.22	0.24	0.75	0.58
IER3	NM_003897	Response to stress	Immediate early response 3	0.20	0.04	0.36	0.17
IFIT1	NM_001548	Response to stimulus	Interferon-induced protein with tetratricopeptide repeats 1	7.02	4.70	2.34	2.14
OASL	NM_003733	Response to stimulus	2'-5'-oligoadenylate synthetase-like	5.98	6.05	3.25	3.58
METTL7A	NM_014033	Methyltransferase	Methyltransferase like 7A	4.28	17.71	4.09	8.86
HERC5	NM_016323	Ubiquitin-protein ligase	Hect domain and RLD 5	6.48	5.99	2.64	2.66
Cell-cell interaction and extracellular matrix remodeling							
GJB5	NM_005268	Gap junction channel activity	Gap junction protein, beta 5	0.20	0.16	0.39	0.23
LAMB3	NM_001127641	Cell-matrix or cell-cell adhesion	Laminin, beta 3	0.21	0.13	0.69	0.23
MMP-1	NM_002421	Metallopeptidase activity	Matrix metallopeptidase 1	0.13	0.03	0.81	0.22
MMP3	NM_002422	Metallopeptidase activity	Matrix metallopeptidase 3	0.13	0.06	0.07	0.01
MMP10	NM_002425	Metallopeptidase activity	Matrix metallopeptidase 10	0.06	0.00	0.22	0.06
MMP12	NM_002426	Metallopeptidase activity	Matrix metallopeptidase 12	0.05	0.02	0.07	0.01
MMP13	NM_002427	Metallopeptidase activity	Matrix metallopeptidase 13	0.22	0.05	0.38	0.23
ITGA2	NM_002203	Cell adhesion molecule	Integrin, alpha 2	0.19	0.03	0.43	0.13
AMIGO2	NM_181847	Extracellular matrix protein	Adhesion molecule with Ig-like domain 2	0.25	0.05	0.24	0.04
Cytoskeleton remodeling and molecular trafficking							
MICAL2	NM_014632	Structural constituent of cytoskeleton	Microtubule associated monooxygenase	0.20	0.14	0.04	0.04
KRT6A	NM_005554	Intermediate filament cytoskeleton	Keratin, type II cytoskeletal 6A	0.13	0.07	0.09	0.02
KRT6B	NM_005555	Intermediate filament cytoskeleton	Keratin, type II cytoskeletal 6B	0.19	0.13	0.12	0.08
DCLK1	NM_004734	Structural constituent of cytoskeleton	Doublecortin-like kinase 1	0.24	0.12	0.03	0.03
TNS4	NM_032865	Actin cytoskeleton	Tensin 4	0.22	0.15	0.27	0.12
MALL	NM_005434	Membrane traffic protein	Mal, T-cell differentiation protein-like	0.24	0.12	0.27	0.11
SLC12A3	NM_000339	Cation transmembrane transporter	Solute carrier family 12 (sodium/chloride transporters), member 3	5.36	29.62	7.03	20.04
SLC44A2	NM_001145056	Transmembrane transporter activity	Solute carrier family 44, member 2	4.74	5.69	2.76	2.90
Inflammation and immunity regulation							
PTGS2	NM_000963	Inflammation and oxidoreductase activity	Prostaglandin-endoperoxide synthase 2	0.14	0.04	0.31	0.08
IL1A	NM_000575	Inflammation mediated by chemokine and cytokine	Interleukin 1, alpha	0.20	0.15	0.16	0.07
IL1B	NM_000576	Inflammation mediated by chemokine and cytokine	Interleukin 1, beta	0.21	0.23	0.14	0.12
Epithelial-mesenchymal transition							
SNAI2	NM_003068	Transcription factor activity	Snail homolog 2 (Drosophila)	0.22	0.13	0.81	0.49



**Table 1.** (Continued)

Symbol	Accession no.	Molecular function <sup>a</sup>	Gene description	FC (array)		FC (qPCR)	
				36 h	48 h	36 h	48 h
Others							
PTHLH	NM_198966	Peptide hormone	Parathyroid hormone-like hormone	0.18	0.11	0.32	0.21
EVI2B	NM_006495	Unclassified	Ecotropic viral integration site 2B	0.19	0.13	0.20	0.05
FAM172B	AK127584	Unclassified	Family with sequence similarity 172, member B pseudogene	0.23	0.19	0.22	0.07
TMEM154	NM_152680	Unclassified	Transmembrane protein 154	0.24	0.09	0.24	0.16
FST	NM_006350	Unclassified	Follistatin	0.20	0.20	0.37	0.37
PHLDA1	NM_007350	Unclassified	Pleckstrin homology-like domain, family A, member 1	0.12	0.05	0.19	0.10

<sup>a</sup>Molecular functions were defined by the GO database (<http://amigo.geneontology.org>) or the Panther classification system (<http://www.pantherdb.org>).

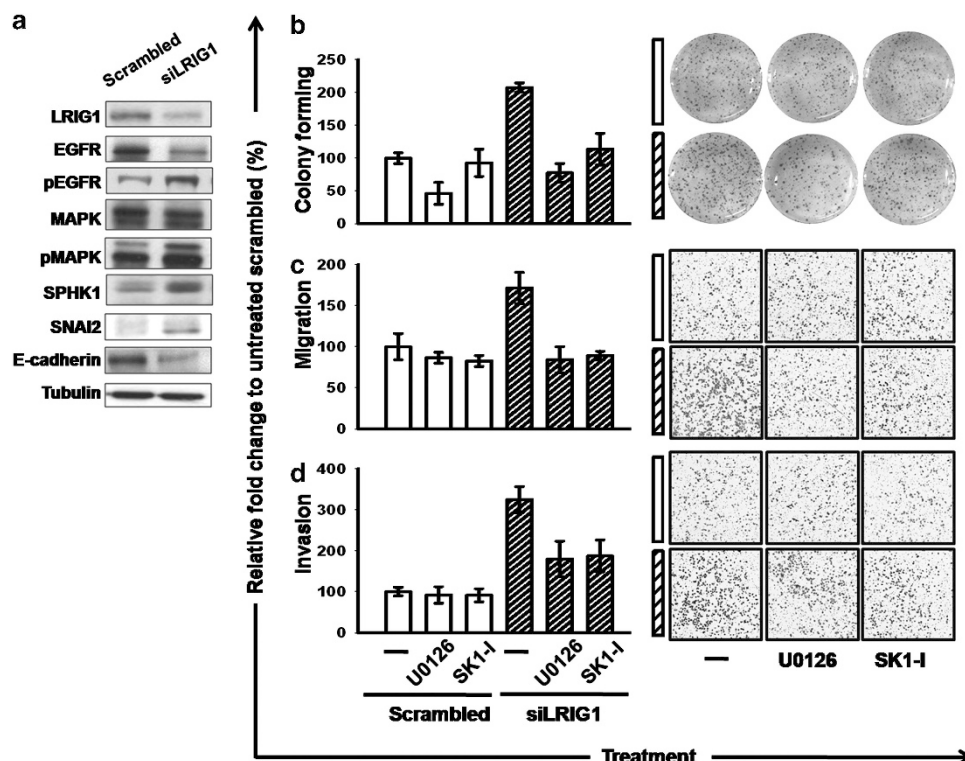


**Figure 5.** LRIG1 knockdown enhances oncogenic properties of head and neck cancer cells. Endogenous LRIG1 were knocked down using siRNA targeted to LRIG1 (siLRIG1). Cells transfected with scrambled siRNA were used as controls. **(a)** Whole cell lysates were harvested 48 h after transfection and western blot analysis for LRIG1, EGFR, pEGFR, MAPK, pMAPK, SPHK1, SNAI2, E-cadherin and alpha-tubulin was carried out. **(b–d)** Inhibitory effects of U0126 (3  $\mu$ M) and SK1-I (3  $\mu$ M) treatment on LRIG1-knocked down cells. **(b)** Clonogenicity was determined by colony formation in soft agar. **(c)** Migration and **(d)** invasiveness of LRIG1-knocked down cells were evaluated by Trans-well and Matrigel-coated Trans-well assay, respectively. Left panels: number of cells in the experimental groups expressed as percentage of that in the untreated scrambled control groups. Right panels: representative images. Results are from at least three independent experiments (mean  $\pm$  s.d.), each with four replicates.

pMAPK or other unidentified transcriptional factors, resulting in further attenuation of EGFR signaling. In addition, the decreased expression of MMPs reduces ECM remodeling activity and inhibits the release of EGFR ligands/activators sequestered by ECM, which also leads to the inhibition of EGFR signaling. Moreover, decreased SPHK1 levels may reduce production of S1P, which binds to G-protein-coupled S1P receptors (S1PRs) that can transactivate other receptor-type tyrosine kinases (RTKs) including EGFR.<sup>27</sup> Thus, increased LRIG1 expression may not only attenuate EGFR-MAPK signaling, but also trigger a positive feedback inhibitory loop that further downregulates EGFR-MAPK-SPHK1 signaling. In contrast, the loss of LRIG1 in NPC cells will lead to tumor aggressiveness as

a consequence of higher activation of EGFR-MAPK-SPHK1 signaling and enhancement of ECM remodeling activity. These findings suggest that MAPK and SPHK1 are potential therapeutic targets for tumors with LRIG1 loss.

SPHK1 catalyzes the conversion of sphingosine to sphingosine-1-phosphate (S1P), a bioactive lipid molecule that mediates S1P signaling by binding to S1P receptors. A handful of studies have shown that various types of human cancers acquire survival advantage, aggressiveness and chemotherapy resistance via non-oncogenic addiction to S1P signaling.<sup>28,29</sup> Because of the overexpression/activation of SPHK1 in cancer cells, SPHK1 has been cited as an emerging target for cancer therapy.<sup>30,31</sup>

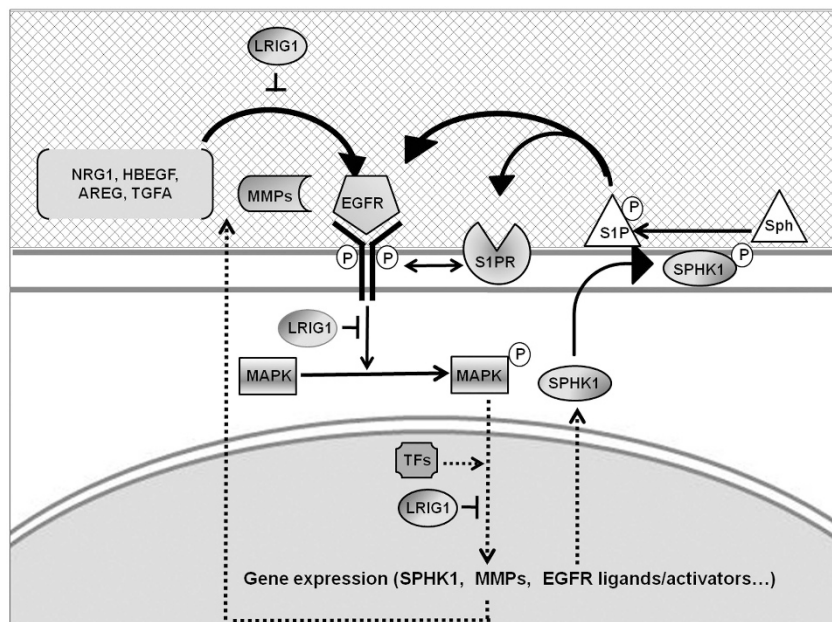


**Figure 6.** Model outlining the role of LRIG1 in a positive feedback inhibitory loop in the regulation of EGFR-MAPK-SPHK1 signaling and ECM remodeling. Sph, sphingosine; S1P, sphingosine-1-phosphate; S1PR, sphingosine 1-phosphate receptor.

Activation of EGFR-MAPK signaling is one of the mechanisms to increase SPHK1 activity, both at the level of expression and phosphorylation.<sup>25</sup> In addition, hyperactivation of EGFR signaling has been linked to the development of head and neck cancers by various approaches including functional genomics, quantitative phosphoproteomics and clinical association studies.<sup>24,32,33</sup> S1P signaling can activate G-protein-coupled S1PRs that subsequently transactivate EGFR in the presence of MMPs and HBEGF.<sup>27</sup> Our findings uncovered a novel reciprocal mechanism of signaling cross-talk between EGFR-MAPK-SPHK1 and S1PR signaling in head and neck cancers, and LRIG1 has a key regulating role in this signaling network (Figure 6).

The signaling strength and duration of EGFR activation are controlled by multiple circuits of positive and/or negative feedback regulation. One such mechanism entails greater MMP activity in the ECM, whereas enhancement of ECM remodeling activity could be accompanied by local release of ECM-sequestered growth factors, cytokines and receptor tyrosine kinase ligands without *de-novo* protein synthesis.<sup>34,35</sup> In head and neck cancers, *EGFR* amplification and *LRIG1* (chromosome 3p) deletion are pathogenic events frequently observed in tumor tissues.<sup>3,5,23</sup> Clinically, both *EGFR* overexpression and *LRIG1* downregulation correlate with a poor clinical outcome;<sup>36</sup> biologically, *LRIG1* acts as a negative regulator to suppress EGFR-MAPK-SPHK1 signaling and ECM remodeling by positive-feedback inhibitory regulation (Figure 6). Our study suggests that low levels of EGFR negative regulators, such as *LRIG1* deletion, may elicit full oncogenic signaling, resulting in a permissive environment for tumor onset and progression.

In addition to its role as negative regulator for EGFR, *LRIG1* was recently identified as a potent stem cell marker for non-cycling, long-lived populations located at the interfollicular epidermis<sup>37,38</sup> or crypt base of the intestine.<sup>39,40</sup> Genetic ablation of *LRIG1* disturbs epithelial homeostasis and increases proliferative capacity of stem cells,<sup>41</sup> which may contribute to tumor formation. These findings raise the possibility that *LRIG1*<sup>-/-</sup> cells harbor a mesenchymal phenotype to promote cancer progression and metastasis in combination with other genetic alterations, which warrants further investigation. Our results showed that the expression of *SNAI2*, an epithelial-to-mesenchymal transition

marker, was induced in *LRIG1* knockdown cells, while the expression of epithelium marker E-cadherin was dramatically reduced (Figure 5a). In agreement with this finding, morphological analyses showed that *LRIG1* controls cell shape/architecture (Figure 4d). As SPHK1-S1P signaling,<sup>42</sup> MMPs and ECM remodeling<sup>43-45</sup> have also been linked to epithelial-to-mesenchymal transition, it will be interesting to investigate how *LRIG1* regulates epithelial-to-mesenchymal transition in promoting aggressive phenotypes, such as metastasis and resistance to radio-/chemotherapy. Furthermore, differential subcellular protein localization or compensatory feedback mechanisms might account for *LRIG1* protein upregulation in some tumor types.<sup>46</sup> This suggests that the subcellular localization of *LRIG1* may determine its function in oncogenesis. The significance of specific subcellular localization of *LRIG1* needs further investigation to elucidate the role of *LRIG1* in human cancer.

In summary, our study suggests novel functions for *LRIG1* in regulating cellular mobility and metastasis via EGFR-MAPK-SPHK1 signaling and ECM remodeling. Through transcriptional regulation and signaling transaction, *LRIG1* is involved in a positive feedback loop that may determine cancer development. Inhibitors of MAPK or SPHK1 signaling components may be considered as candidate drugs for treating patients whose tumors show chromosome 3p/*LRIG1* loss.

## MATERIALS AND METHODS

### Cell lines and reagents

Inhibitors U0126 and SKI-I (BML-258) were purchased from Sigma (St Louis, MO, USA) and Enzo Life Sciences (Farmingdale, NY, USA), respectively. Two established human NPC cell lines, TW01 and TW06,<sup>47</sup> were used in this study and cultured in Dulbecco's minimal essential medium containing 10% fetal calf serum at 37 °C under 5% CO<sub>2</sub>. Immunohistochemistry and western blot was performed using antibodies against human *LRIG1* (Abcam, Cambridge, UK), *EGFR*, p-EGFR(1068Y) or *SNAI2* (Cell Signaling, Danvers, MA, USA), MAPK and phospho-MAPK (pMAPK) (Merck Millipore, Billerica, MA, USA), SPHK1 (Abnova, Taipei, Taiwan), single-stranded DNA (ssDNA) (ENZO Life Sciences), integrin-β1 or GAPDH or α-tubulin (Santa Cruz Biotechnology, Santa Cruz, CA, USA). ECM proteins including MMP-1, -2, -3, -8, -9, -10 and



-13, and their inhibitors TIMP-1, -2, and -4 were measured by antibody array (RayBio MMP human array 1, RayBiotech, Norcross, GA, USA) following the manufacturer's protocol and quantified on an ImageQuant LAS4000 (GE Healthcare Life Sciences, Pittsburgh, PA, USA).

#### Human tumor tissues and immunohistochemistry

Tissue microarrays containing samples of forty-four metastatic NPC tissues and two normal oral epithelia were described previously.<sup>3</sup> Four representative cores from each formalin-fixed paraffin-embedded tumor were arranged on tissue microarrays for immunohistochemistry.

#### Statistical analysis and clinical correlation

Clinical information about NPC samples analyzed in this study, including tumor site, clinical stage, treatment history, recurrent status and five-year survival, was collected from clinical notes. The overall survival time was defined as the number of months between diagnosis and death or between diagnosis and the most recent follow-up. All calculations and statistical analyses were carried out using the SAS/STAT software package (SAS Institute, Cary, NC, USA) and plotted as survival curves using the Kaplan–Meier method. With this method, *P*-values <0.05 were considered significant.

#### Quantitative real-time PCR

The PCR primers were designed by the Universal Probe Library Assay Design Center (<https://www.roche-applied-science.com>). Quantitative real-time PCR was carried out on an ABI 7900HT sequence detection system (Applied Biosystems, Carlsbad, CA, USA) using a FastStart Universal Probe Master Kit (Roche Applied Science, Indianapolis, IN, USA). Fold changes in expression of target genes in the experimental sample relative to that in the control sample were calculated by normalization to ACTB or GAPDH levels.

#### Transfection and siRNA knockdown

LRIG1 was knocked down in TW06 cells by Dharmacon ON-TARGET plus SMART pool (Dharmacon, Lafayette, CO, USA), with ON-TARGET plus siCONTROL non-targeting pool as the control. Cells were transiently transfected with 100 nm siRNA using Turbofect (Fermentas/Thermo Scientific, Waltham, MA, USA); then, the medium was replaced 8 h after transfection and the cells were incubated for a further 16–24 h.

#### Generation of stable LRIG1-inducible clones

An inducible system was generated in TW01 cells by transfection with tetracycline-controlled transactivator (tTA) expression vector. Full-length LRIG1 cDNA (tagged with V5 at C-terminus) was cloned into a pBI-inducible vector (Clontech, Mountain View, CA, USA), and these expression vectors were subsequently introduced into TW01 cells. For controls, the empty vector was introduced into TW01-tTA cells. Two TW01 transfectants, TW01-LG1/a and TW01-LG1/b, were generated by selection with G418 and hygromycin. Ectopic expression of LRIG1 was controlled by tetracycline-responsive element in the promoter, with the genes being turned on in a doxycycline-free and turned off in a doxycycline-containing medium. Cell clones were validated by western blot and immunostaining.

#### Tumor xenografts in nude mice

LRIG1-inducible TW01-LG1/a cells were injected subcutaneously into athymic *nu/nu* mice ( $5 \times 10^6$  cells per injection, two injection sites per mouse, five mice per group). The LRIG1 turned-off control mice were injected intraperitoneally with doxycycline (125 µg/mouse) every day to suppress LRIG1 expression, while the LRIG1 turned-on group was injected with the same volume of phosphate-buffered saline. Tumor volume was measured every 3 days, and tumors were excised and weighed on Day 43.

#### Microarray analysis

Cellular RNA was harvested using an RNeasy kit (Qiagen, Germantown, MD, USA) according to the manufacturer's instructions. A WT cDNA Synthesis Kit and WT Terminal Labeling Kit (Affymetrix, Santa Clara, CA, USA) were used to generate amplified and labeled sense cDNA. The cDNA was hybridized to the Affymetrix Human Gene 1.0 ST Array according to standard Affymetrix protocol. Washing and staining steps were carried out using a GeneChip Fluidics station FS 450, and slides were scanned with an Affymetrix Gene Chip scanner 3000 7G system. Raw data were imported

and analyzed by GeneSpring GX (Agilent Technologies, Santa Clara, CA, USA) to generate gene lists of differentially expressed (fold change in expression >2). Microarray data have been deposited in the National Center for Biotechnology Information's Gene Expression Omnibus (GEO), and are accessible through GEO with the accession number GSE37349 (<http://www.ncbi.nlm.nih.gov/geo/query/acc.cgi?acc=GSE37349>).

#### Chromatin immunoprecipitation (ChIP) assay

LRIG1-inducible TW01 cells after the gene being turned-on or turned-off were fixed by addition of 1% formaldehyde to culture medium, and cells were lysed on ice with RIPA buffer (Sigma) containing protease inhibitors (Roche, Basel, Switzerland). Genomic DNA was fragmented by sonication to sizes ranging from 200–500 bp, then 1 µg of the fragments was incubated overnight at 4 °C with gentle rotation with 2 µl of anti-phospho-MAKP antibodies (ab50011 from Abcam) and 50 µl of protein A/G beads (Sigma). Then, protein–DNA complexes on beads were washed with RIPA buffer before elution with 1% SDS and 50 mM NaHCO<sub>3</sub>. ChIP-PCR for promoter regions of candidate genes was performed with primers shown in Supplementary Table 1.

#### Cell viability and proliferation assays

Cells ( $1 \times 10^4$  cells per well) were seeded overnight in 24-well plates, then placed in medium for the indicated time, then cell numbers were quantified by MTT assay. Briefly, MTT was added to cells at a final concentration of 0.5 mg/ml, then the cells were incubated at 37 °C for 3 h and lysed with DMSO, and the amount of formazan in each well was determined colorimetrically at 570 nm, using a spectrophotometer (Molecular Devices, Sunnyvale, CA, USA). Data from three independent experiments, each with four replicates, were averaged.

#### Morphology assay

Collagen-coated dish was prepared for morphology assay as described previously.<sup>48</sup> Briefly, tissue culture dishes (BD Biosciences, San Jose, CA, USA) were coated with 5 µg/ml of collagen Type I (BD Biosciences) in 0.02 N glacial acetic acid at 4 °C overnight, then the coating solution was aspirated out. The coated plate was washed with PBS once before use. TW01-LG1/a cells were seeded at a density of  $2 \times 10^6$  cells in 10-cm plates. After adhesion, cells were cultured in doxycycline-containing (LRIG1-off) or doxycycline-free medium (LRIG1-on). Phase-contrast pictures were taken every 24 h after turn on LRIG1 expression.

#### Soft agar assay

Cells were resuspended in culture medium containing 0.3% agarose at a density of  $1 \times 10^5$  cells in 6-well plates, then overlaid with 0.6% agarose and fed with fresh medium weekly for 3 weeks. After fixation and staining with violet blue, colonies were photographed and quantified using MetaMorph software (Molecular Devices). The experiment was performed three times, each time with four replicates.

#### Cell migration and invasion assays

An *in-vitro* cell migration assay was carried out using Trans-well chambers (8 µm pore size, BD Biosciences). For cell invasion assay, the chambers were coated with Matrigel (BD Biosciences). Cells were plated at a density of  $5 \times 10^4$  cells per chamber in a 24-well plate in serum-free Dulbecco's minimal essential medium in the top chamber according to the manufacturer's instructions, and Dulbecco's minimal essential medium containing 10% FCS was placed in the bottom chamber as the chemoattractant. After 24 h, cells that had migrated into, or invaded, the bottom chambers were stained with crystal violet and counted in four random fields using MetaMorph software (Molecular Devices). Data were averaged for three independent experiments, each with four replicates.

#### CONFLICT OF INTEREST

The authors declare no conflict of interest.

#### ACKNOWLEDGEMENTS

We thank Dr Mien-Chie Hung (MD Anderson Cancer Center, TX, USA) and Dr Yosef Yarden (Weizmann Institute, Israel) for their critical comments on this study, which was supported by grants from the National Science Council, Taiwan (NSC99-2320-B-400-

009, NSC100-2325-B-400-014, NSC101-2320-B-039-006 and NSC101-2320-B-039-006), the National Health Research Institutes, Taiwan (CA-101-PP-01), China Medical University Hospital, Taiwan (DMR99-047), and the Department of Health, Taiwan (DOH101-TD-C-111-004 and DOH101-TD-C-111-005).

## REFERENCES

- Pai SI, Westra WH. Molecular pathology of head and neck cancer: implications for diagnosis, prognosis, and treatment. *Ann Rev Pathol* 2009; **4**: 49–70.
- Fang CY, Lee CH, Wu CC, Chang YT, Yu SL, Chou SP et al. Recurrent chemical reactivations of EBV promotes genome instability and enhances tumor progression of nasopharyngeal carcinoma cells. *Int J Cancer* 2009; **124**: 2016–2025.
- Sheu JJ, Lee CH, Ko JY, Tsao GS, Wu CC, Fang CY et al. Chromosome 3p12.3-p14.2 and 3q26.2-q26.32 are genomic markers for prognosis of advanced nasopharyngeal carcinoma. *Cancer Epidemiol Biomarkers Prev* 2009; **18**: 2709–2716.
- Maseki S, Ijichi K, Tanaka H, Fujii M, Hasegawa Y, Ogawa T et al. Acquisition of EMT phenotype in the gefitinib-resistant cells of a head and neck squamous cell carcinoma cell line through Akt/GSK-3beta/snail signalling pathway. *Br J Cancer* 2012; **106**: 1196–1204.
- Jin Y, Jin C, Lv M, Tsao SW, Zhu J, Wennerberg J et al. Karyotypic evolution and tumor progression in head and neck squamous cell carcinomas. *Cancer Genet Cytogenet* 2005; **156**: 1–7.
- Koy S, Plaschke J, Luksch H, Friedrich K, Kuhlisch E, Eckelt U et al. Microsatellite instability and loss of heterozygosity in squamous cell carcinoma of the head and neck. *Head Neck* 2008; **30**: 1105–1113.
- Huang Z, Desper R, Schaffer AA, Yin Z, Li X, Yao K. Construction of tree models for pathogenesis of nasopharyngeal carcinoma. *Genes Chromosomes Cancer* 2004; **40**: 307–315.
- Hedman H, Nilsson J, Guo D, Henriksson R. Is LRIG1 a tumour suppressor gene at chromosome 3p14.3? *Acta Oncol* 2002; **41**: 352–354.
- Thomasson M, Hedman H, Guo D, Ljungberg B, Henriksson R. LRIG1 and epidermal growth factor receptor in renal cell carcinoma: a quantitative RT–PCR and immunohistochemical analysis. *Br J Cancer* 2003; **89**: 1285–1289.
- Lindstrom AK, Ekman K, Stendahl U, Tot T, Henriksson R, Hedman H et al. LRIG1 and squamous epithelial uterine cervical cancer: correlation to prognosis, other tumor markers, sex steroid hormones, and smoking. *Int J Gynecol Cancer* 2008; **18**: 312–317.
- Stutz MA, Shattuck DL, Laederich MB, Carraway 3rd KL, Sweeney C. LRIG1 negatively regulates the oncogenic EGF receptor mutant EGFRvIII. *Oncogene* 2008; **27**: 5741–5752.
- Miller JK, Shattuck DL, Ingalla EQ, Yen L, Borowsky AD, Young LJ et al. Suppression of the negative regulator LRIG1 contributes to ErbB2 overexpression in breast cancer. *Cancer Res* 2008; **68**: 8286–8294.
- Ljuslinder I, Golovleva I, Henriksson R, Grankvist K, Malmer B, Hedman H. Co-incidental increase in gene copy number of ERBB2 and LRIG1 in breast cancer. *Breast Cancer Res* 2009; **11**: 403.
- Jensen KB, Jones J, Watt FM. A stem cell gene expression profile of human squamous cell carcinomas. *Cancer Lett* 2008; **272**: 23–31.
- Krig SR, Frieze S, Simion C, Miller JK, Fry WH, Rafidi H et al. Lrig1 is an estrogen-regulated growth suppressor and correlates with longer relapse-free survival in ERalpha-positive breast cancer. *Mol Cancer Res* 2011; **9**: 1406–1417.
- Gur G, Rubin C, Katz M, Amit I, Citri A, Nilsson J et al. LRIG1 restricts growth factor signaling by enhancing receptor ubiquitylation and degradation. *EMBO J* 2004; **23**: 3270–3281.
- Yi W, Holmlund C, Nilsson J, Inui S, Lei T, Itami S et al. Paracrine regulation of growth factor signaling by shed leucine-rich repeats and immunoglobulin-like domains 1. *Exp Cell Res* 2011; **317**: 504–512.
- Goldoni S, Izzo RA, Kay P, Campbell S, McQuillan A, Agnew C et al. A soluble ectodomain of LRIG1 inhibits cancer cell growth by attenuating basal and ligand-dependent EGFR activity. *Oncogene* 2007; **26**: 368–381.
- Laederich MB, Funes-Duran M, Yen L, Ingalla E, Wu X, Carraway 3rd KL et al. The leucine-rich repeat protein LRIG1 is a negative regulator of ErbB family receptor tyrosine kinases. *J Biol Chem* 2004; **279**: 47050–47056.
- Ye F, Gao Q, Xu T, Zeng L, Ou Y, Mao F et al. Upregulation of LRIG1 suppresses malignant glioma cell growth by attenuating EGFR activity. *J Neurooncol* 2009; **94**: 183–194.
- Shattuck DL, Miller JK, Laederich M, Funes M, Petersen H, Carraway 3rd KL et al. LRIG1 is a novel negative regulator of the Met receptor and opposes Met and Her2 synergy. *Mol Cell Biol* 2007; **27**: 1934–1946.
- Ledda F, Bieraugel O, Fard SS, Vilar M, Paratcha G. Lrig1 is an endogenous inhibitor of Ret receptor tyrosine kinase activation, downstream signaling, and biological responses to GDNF. *J Neurosci* 2008; **28**: 39–49.
- Abhold EL, Kiang A, Rahimy E, Kuo SZ, Wang-Rodriguez J, Lopez JP et al. EGFR kinase promotes acquisition of stem cell-like properties: a potential therapeutic target in head and neck squamous cell carcinoma stem cells. *PLoS One* 2012; **7**: e32459.
- Sheu JJ, Hua CH, Wan L, Lin YJ, Lai MT, Tseng HC et al. Functional genomic analysis identified epidermal growth factor receptor activation as the most common genetic event in oral squamous cell carcinoma. *Cancer Res* 2009; **69**: 2568–2576.
- Pitson SM, Moretti PA, Zebol JR, Lynn HE, Xia P, Vadas MA et al. Activation of sphingosine kinase 1 by ERK1/2-mediated phosphorylation. *EMBO J* 2003; **22**: 5491–5500.
- Chang SJ, Wang TY, Lee YH, Tai CJ. Extracellular ATP activates nuclear translocation of ERK1/2 leading to the induction of matrix metalloproteinases expression in human endometrial stromal cells. *J Endocrinol* 2007; **193**: 393–404.
- Shida D, Kitayama J, Yamaguchi H, Yamashita H, Mori K, Watanabe T et al. Sphingosine 1-phosphate transactivates c-Met as well as epidermal growth factor receptor (EGFR) in human gastric cancer cells. *FEBS Lett* 2004; **577**: 333–338.
- Pyne NJ, Pyne S. Sphingosine 1-phosphate and cancer. *Nat Rev Cancer* 2010; **10**: 489–503.
- Pyne NJ, Tonelli F, Lim KG, Long JS, Edwards J, Pyne S. Sphingosine 1-phosphate signalling in cancer. *Biochem Soc Trans* 2012; **40**: 94–100.
- Pyne S, Bittman R, Pyne NJ. Sphingosine kinase inhibitors and cancer: seeking the golden sword of Hercules. *Cancer Res* 2011; **71**: 6576–6582.
- Shida D, Takabe K, Kapitonov D, Milstien S, Spiegel S. Targeting SphK1 as a new strategy against cancer. *Curr Drug Targets* 2008; **9**: 662–673.
- Ma BB, Poon TC, To KF, Zee B, Mo FK, Chan CM et al. Prognostic significance of tumor angiogenesis, Ki 67, p53 oncoprotein, epidermal growth factor receptor and HER2 receptor protein expression in undifferentiated nasopharyngeal carcinoma—a prospective study. *Head Neck* 2003; **25**: 864–872.
- Ruan L, Li XH, Wan XX, Yi H, Li C, Li MY et al. Analysis of EGFR signaling pathway in nasopharyngeal carcinoma cells by quantitative phosphoproteomics. *Proteome Sci* 2011; **9**: 35.
- Munger JS, Sheppard D. Cross talk among TGF-beta signaling pathways, integrins, and the extracellular matrix. *Cold Spring Harb Perspect Biol* 2011; **3**: a005017.
- Gaide Chevrionnay HP, Selvais C, Emonard H, Galant C, Marbaix E, Henriot P. Regulation of matrix metalloproteinases activity studied in human endometrium as a paradigm of cyclic tissue breakdown and regeneration. *Biochim Biophys Acta* 2012; **1824**: 146–156.
- Burtne B. The role of cetuximab in the treatment of squamous cell cancer of the head and neck. *Expert Opin Biol Ther* 2005; **5**: 1085–1093.
- Jensen KB, Collins CA, Nascimento E, Tan DW, Frye M, Itami S et al. Lrig1 expression defines a distinct multipotent stem cell population in mammalian epidermis. *Cell Stem Cell* 2009; **4**: 427–439.
- Watt FM, Jensen KB. Epidermal stem cell diversity and quiescence. *EMBO Mol Med* 2009; **1**: 260–267.
- Powell AE, Wang Y, Li Y, Poulin EJ, Means AL, Washington MK et al. The pan-ErbB negative regulator Lrig1 is an intestinal stem cell marker that functions as a tumor suppressor. *Cell* 2012; **149**: 146–158.
- Wong VW, Stange DE, Page ME, Buczaczi S, Wabik A, Itami S et al. Lrig1 controls intestinal stem-cell homeostasis by negative regulation of ErbB signalling. *Nat Cell Biol* 2012; **14**: 401–408.
- Ordóñez-Moran P, Huelsken J. Lrig1: a new master regulator of epithelial stem cells. *EMBO J* 2012; **31**: 2064–2066.
- Milara J, Navarro R, Juan G, Peiro T, Serrano A, Ramon M et al. Sphingosine-1-phosphate is increased in patients with idiopathic pulmonary fibrosis and mediates epithelial to mesenchymal transition. *Thorax* 2012; **67**: 147–156.
- Lochter A, Galosy S, Muschler J, Freedman N, Werb Z, Bissell MJ. Matrix metalloproteinase stromelysin-1 triggers a cascade of molecular alterations that leads to stable epithelial-to-mesenchymal conversion and a premalignant phenotype in mammary epithelial cells. *J Cell Biol* 1997; **139**: 1861–1872.
- Song W, Jackson K, McGuire PG. Degradation of type IV collagen by matrix metalloproteinases is an important step in the epithelial-mesenchymal transformation of the endocardial cushions. *Dev Biol* 2000; **227**: 606–617.
- Radisky ES, Radisky DC. Matrix metalloproteinase-induced epithelial-mesenchymal transition in breast cancer. *J Mammary Gland Biol Neoplasia* 2010; **15**: 201–212.
- Hedman H, Henriksson R. LRIG inhibitors of growth factor signalling—double-edged swords in human cancer? *Eur J Cancer* 2007; **43**: 676–682.
- Lin CT, Wong CI, Chan WY, Tzung KW, Ho JK, Hsu MM et al. Establishment and characterization of two nasopharyngeal carcinoma cell lines. *Lab Invest* 1990; **62**: 713–724.
- Chang H, Shyu KG, Lin S, Wang BW, Liu YC, Lee CC. Cell adhesion induces the plasminogen activator inhibitor-1 gene expression through phosphatidylinositol 3-kinase/Akt activation in anchorage dependent cells. *Cell Commun Adhes* 2002; **9**: 239–247.

Supplementary Information accompanies this paper on the Oncogene website (<http://www.nature.com/onc>)